JOURNAL OF SOLID STATE CHEMISTRY 50, 321–334 (1983)

Electron Microscopy Studies of Modulated Structures in (Au, Ag)Te_2: Part I. Calaverite $AuTe_2$

G. VAN TENDELOO, P. GREGORIADES,* AND S. AMELINCKX†

Rijksuniversitair Centrum Antwerpen, Groenenborgerlaan 171, B-2020 Antwerp, Belgium

Received June 6, 1983

Calaverite ($AuTe_2$) has an incommensurate modulated structure in a wide temperature range. This can be deduced from the electron diffraction patterns and from the high resolution images. The main displacements in the modulation wave are along the [010] direction, but there are also displacements parallel with the (010) plane for the tellurium atoms. The unit mesh of the tellurium displacement pattern has only half the size of that of the gold pattern. Substituting tellurium by selenium changes the $\vec{q}$ vector of the modulation.

1. Introduction

The pseudo-binary system (Au, Ag)Te_2 is of some interest since it is possible to substitute up to 50% of the gold atoms in $AuTe_2$ by silver atoms, which have approximately the same atomic size as gold, without changing fundamentally the basic structure; the resulting superstructures depend on the exact composition however. It is the purpose of this paper to study these superstructures by means of electron diffraction and high resolution electron microscopy for different gold/silver ratios. From the limited amount of X-ray diffraction work on natural crystals, there are some vague indications that some of these materials may exhibit modulated structures (*1*). More recently the existence of a modulated structure in calaverite was deduced from X-ray evidence by Sueno *et al.* (*2*).

* On leave from University of Thessaloniki, Greece.

† Also at SCK–CEN, Boeretang, B-2400 Mol, Belgium.

2. Materials and Specimen Preparation

The materials were prepared by melting together the constituent elements in evacuated quartz tubes at 550°C followed by slow cooling over several days. We prepared materials with several compositions; their crystallographic data as determined by Tunell and Pauling (*1*) are summarized in Table I.

Specimens for electron microscopy are prepared by crushing fragments of the ingots. Whereas sylvanite and krennerite have well developed cleavage planes; this is not the case for calaverite. In the first two substances the crystal fragments are preferentially parallel to the cleavage planes, and the best images are obtained along the zone perpendicular to such plane.

3. The Crystal Structure

The crystal structures of calaverite ($AuTe_2$), sylvanite ($AuAgTe_4$), and krennerite ($Au_{0.8}Ag_{0.2}Te_2$) have been deter-

0022-4596/83 $3.00

TABLE I

	Space Group	A_0 (nm)	b_0 (nm)	c_0 (nm)	β
Calaverite	*C2/m*	0.719	0.440	0.507	90°13′
Krennerite	*Pma*	1.654	0.882	0.446	
Sylvanite	*P2/c*	0.896	0.449	1.462	145°26′

mined by Tunell and Pauling (*1*). The simplest among these structures is that of calaverite; in Part I of the paper we limit our discussion to this phase; subsequent papers will be devoted to sylvanite and krennerite.

Calaverite is a somewhat deformed version of the CdI_2 structure, the symmetry being monoclinic. The Van der Waals gap is smaller than in the CdI_2 structure; this is the reason why a pronounced cleavage is not observed in $AuTe_2$. Alternatively it can also be considered as a superstructure based on a slightly deformed primitive cubic lattice with $a \simeq 0.3$ nm. The schematic representation of Fig. 1 is a projection on a 110-type plane of the quasi-cubic lattice, i.e., along the [010] direction of the monoclinic structure. Along this zone the structure is a "column structure" in the sense defined previously (*3*), i.e., all columns contain one atomic species only. This is an important feature when imaging under high resolution conditions.

When viewed along the $[\bar{1}01]$ direction the structure can be considered as consisting of parallel columns, all having the composition $AuTe_2$. The projections of these columns form a very slightly deformed square array; this projection looks in fact similar for the three structures, if one ignores the difference between gold and silver.

One family of "close packed" planes in calaverite is parallel with the *c* planes. When viewed along a direction perpendicular to such planes the projected structure looks close packed, the six first neighbors of a gold column consisting of tellurium columns and the second nearest neighbors of gold columns. Since the structure is pseudo-cubic there are four families of pseudo-close packed planes which are no longer equivalent in the monoclinic calaverite phase; they are (001), $(22\bar{1})$, $(\bar{2}21)$, and (401) and there are four pseudo hexagonal diffraction patterns: [001], [201], $[13\bar{1}]$, and $[\bar{1}31]$.

4. Reciprocal Lattice and Diffraction Pattern

In this section we describe the relevant diffraction patterns, which are in agreement with the reciprocal lattice of the idealized calaverite structure as determined by Tunell and Pauling (*1*). In a later section we shall consider the observed deviations from these patterns and discuss the relations of these with the finer details of the structure.

4.1. Ideal Structure

Three sections of reciprocal space are represented in Fig. 2. The first section (2a) corresponds to the zone along which the projection of Fig. 1 was made, i.e., along [010]. The pattern is almost perfectly rec-

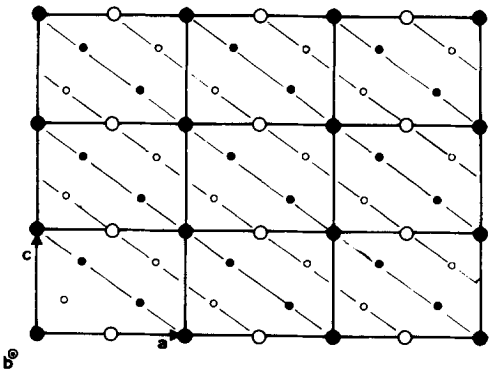

FIG. 1. Structure of calaverite projected along [010]. Large circles represent Au atoms. Open circles are at $y = \frac{1}{2}$ while filled circles are at $y = 0$. The unit cell is outlined and the same convection as in (*1*) is used. Fine dotted lines indicate (202) planes which are nearly perpendicular to the modulation vector.

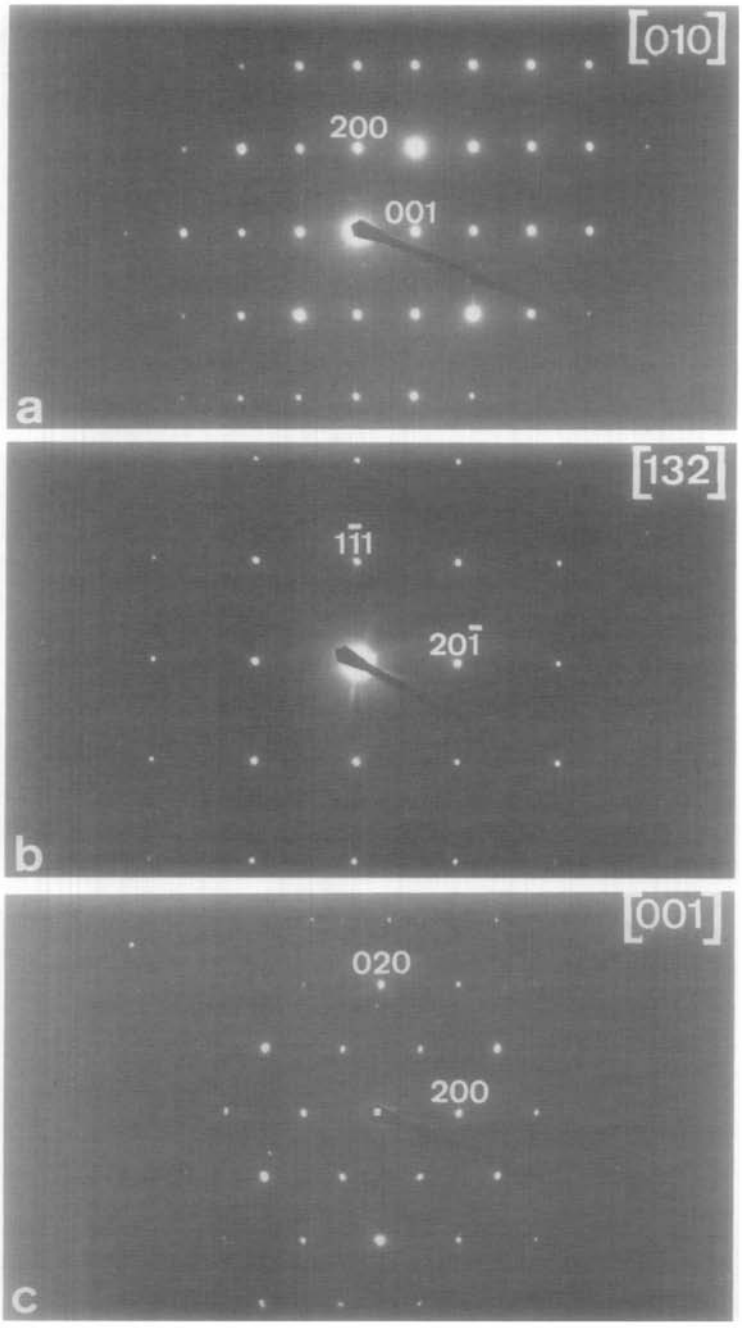

FIG. 2. Three diffraction patterns of $AuTe_2$ showing almost no deviations from the calaverite structure according to Ref. (*1*). (a) [010] (a distorted $(110)_{cubic}$ section); (b) [132] (a basal $(100)_{cubic}$ section); (c) [001] (a pseudo $(111)_{cubic}$ section).

tangular: the lattice is thus pseudo-orthorhombic; this zone corresponds to a ⟨110⟩-type direction of the primitive quasi-cubic lattice.

Figure 2b represents a section along a zone which is parallel with the cube direction of this primitive quasi-cubic lattice. The pattern deviates very little from a square grid. There are in fact three pseudo-cubic sections, which are slightly different one from the other.

Finally, Fig. 2c represents the zone perpendicular to one of the "pseudo-close packed" planes of the deformed cadmium iodide structure; this pattern is very nearly hexagonal. A large number of further sections were obtained, which were all found to be in agreement with the reciprocal lattice of the ideal structure, at least when ignoring the deviations to be discussed in the next paragraph.

4.2. Deviations from the Simple Pattern

In calaverite, sequences of satellite reflections are prominently observed in most sections. The ratio of the intensity of the satellite spots to that of the basic spots from which they are derived increases with increasing length of the diffraction vector. This behavior is typical of deformation modulated structures.

In the $[13\bar{1}]$ zone, perpendicular to pseudo-close packed planes, linear sequences of satellite spots are observed dividing the shortest distance between the basic spots in a nonintegral number of parts, approximately 4.5 (Fig. 3a). Also the orientation of the sequence is not exactly along the direction of close packed rows of basic spots, i.e., the $[202]^*$ direction; there is thus a spacing as well as an orientation anomaly and the resulting pattern is incommensurate.

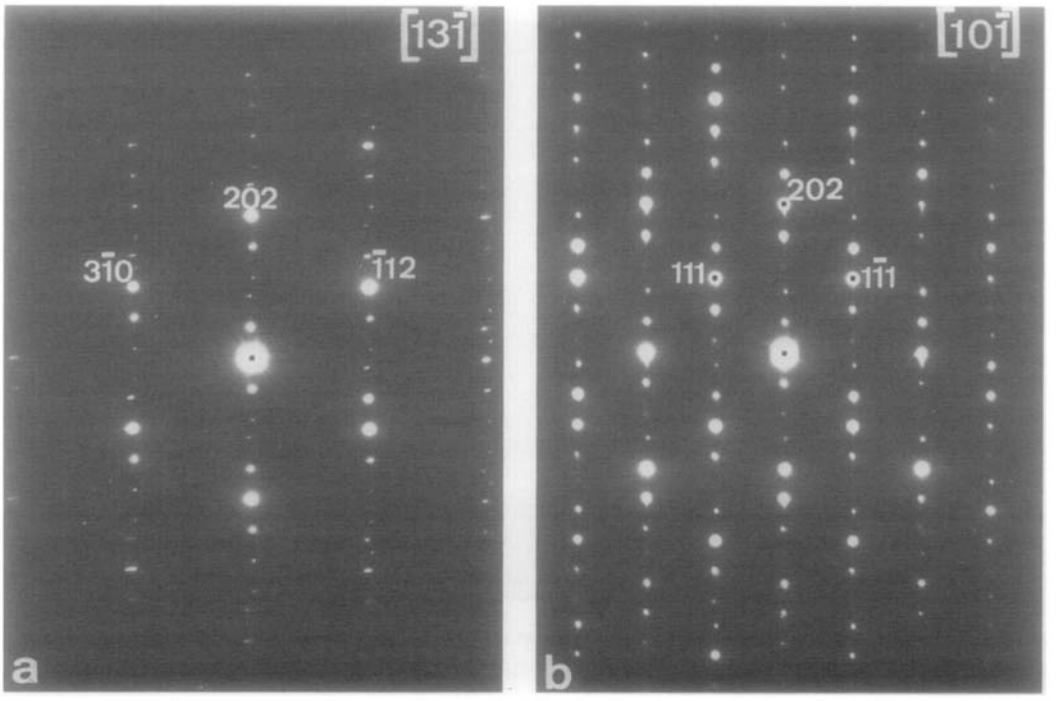

FIG. 3. (a) $[13\bar{1}]$ diffraction pattern (a pseudo-hexagonal section) clearly showing satellite sequences forming an incommensurate diffraction pattern; (b) $[10\bar{1}]$ zone (a pseudo-cubic section) exhibiting the same sequences of satellites.

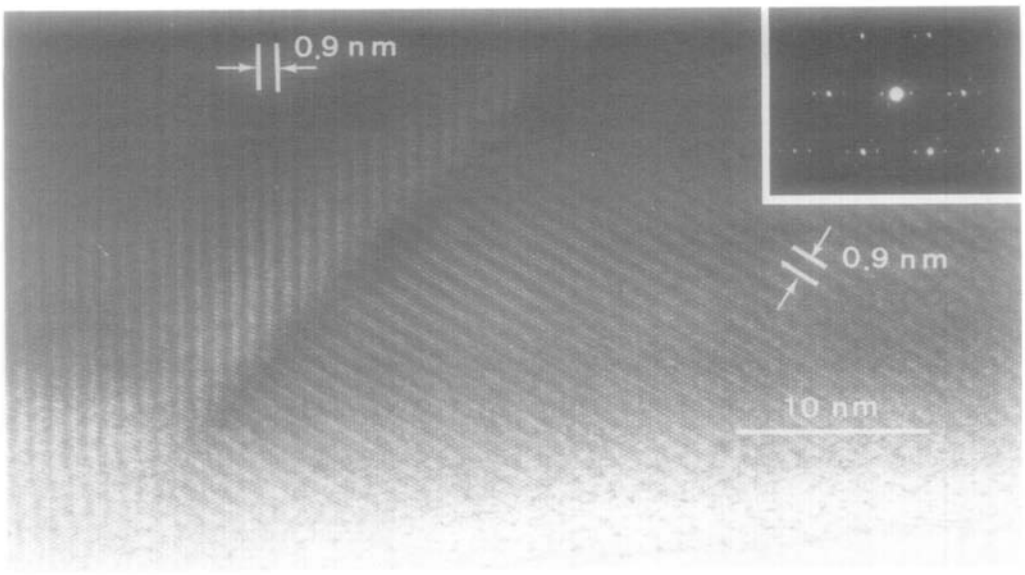

FIG. 4. Two orientation variants of the modulated structure, the two modulation directions differing very roughly 60° in orientation. The diffraction pattern is shown as an inset.

The linear sequences of satellites in this section may occur in two directions differing roughly 60° in orientation; they correspond to two orientation variants of the structure (Fig. 4). The pattern of basic spots is common to both variants; only the sequences of satellites differ 60° in orientation. This suggests that the basic structure is also common, only the modulation being different.

The $[10\bar{1}]$ section also shows the modulation quite pronounced (Fig. 3b). In this pseudo-cubic pattern it is even hard to recognize the original calaverite reflections. It confirms that the modulation is very nearly along $[202]^*$ with a wavelength of approximately 4.5 d_{202}.

In the [010] zone weak reflections are observed (Fig. 2a) as represented more clearly in Fig. 5a. For orientations slightly away from the exact zone orientation (Fig. 5b) the intensity of the satellites increases and spots further away from the basic spots are revealed. This seems to suggest that either the satellite sequences are not precisely in the $(010)^*$ plane or that their intensity is very orientation sensitive.

The analysis of this [010] zone diffraction pattern is somewhat ambiguous; in particular the allocation of satellite spots to basic spots is somewhat arbitrary. In this zone pairs of strong satellite spots are found; they are centered on basic spots with h = odd, which are systematically absent. Furthermore satellite spots are associated with all basic spots with h = even; these are presumably due to double diffraction since their intensity is proportional to that of the basic spots with which they are associated. The vectors leading from the basic spots to the closest satellites are parallel and equal in magnitude with those connecting the pairs of spots.

One can construct different linear sequences of satellite spots derived from basic spots and corresponding with different wavevectors $\bar{\mathbf{q}}$ for the modulation waves: they are represented schematically in Fig. 6. The shortest wavevector corresponds to $\bar{q}_1$; it is implicitly based on the assumption

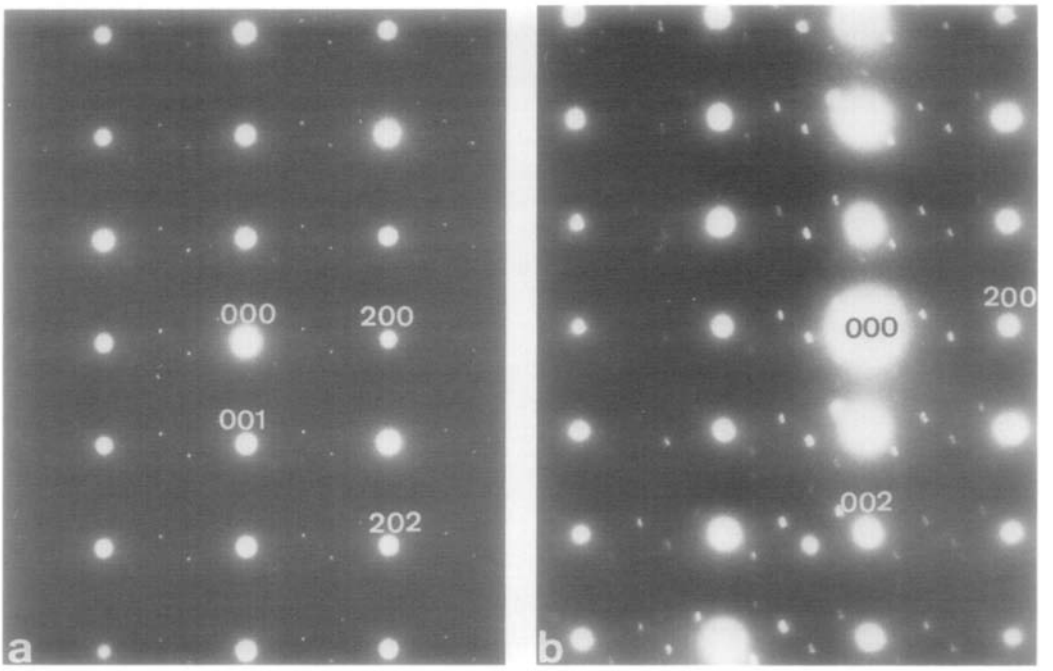

FIG. 5. (a) Overexposed [010] diffraction pattern showing quite clearly the satellite pairs around the position with h = odd; (b) Slightly tilted [010] section; the satellites are enhanced.

that the absent spot h = odd is split; q_1 would be very nearly in the [201]* direction; it would correspond with a wavelength of about 1.43 nm.

The next shortest wavevector would be $\bar{q}_2$; it would enclose a small angle with the [200] direction, the nearest crystallographic direction being $[\bar{8}01]^*$ and the wavelength 0.85 nm. Wavevector $\bar{q}_3$ along [801]* would lead to a wavelength of 0.60 nm. The other conceivable wavevectors are already so large that they would lead to modulation wavelengths of about the same magnitude as the lattice parameter or smaller. From tilting experiments about the [202]* rotation axis, it was found that in the higher levels of the reciprocal lattice, in particular for $h1l$ spots, sequences of satellites appear approximately in the [202]* direction, with the same geometry as that observed in the other sections, i.e., with the same spacing and orientation anomaly (see Fig. 3). It is therefore reasonable to assume that also in the [010] zone the same satellite sequences should be present in the [202]* direction since this direction belongs to the zone unless extinction would make it disappear. Alternatively it is found that on tilting away from the $[13\bar{1}]$ zone about the [202]* axis the first order satellites disappear at the $h0l$ spots wherever they cannot be produced by double diffraction. This leads us to suspect that the observed intense satellite pairs in [010] are in fact the second order satellites, the first order satellites being extinguished in the [010] zone pattern. The sites of the first order satellites are indicated by open circles in Fig. 6. With this assumption the satellite configurations in all sections of reciprocal space can be accounted for in a consistent manner on the basis of a single satellite sequence; this is in particular visible in Figs. 3a and b. The presence of first order satellites (marked by triangles in Fig.

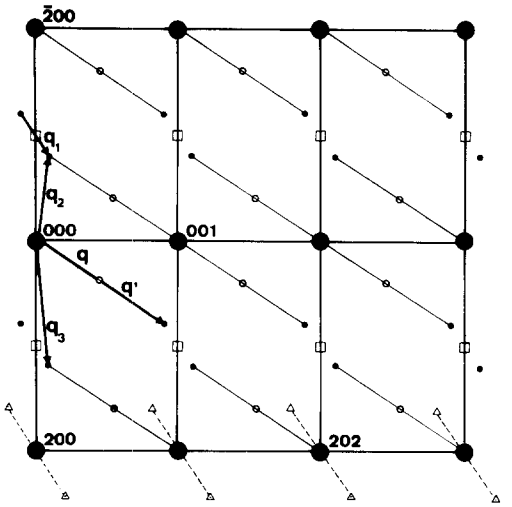

FIG. 6. Schematic [010] diffraction pattern. Basic calaverite reflections are represented as large dots while the observed satellites are indicated by small black dots. The open circles represent structurally forbidden first order satellites while the open squares are at the structurally forbidden but commensurate positions with h = odd. The open triangles (only indicated at the h = 2 row) show the double diffraction spots observed in Fig. 5b. They could also be the fourth order spots of q'.

6) associated with $h0l$ spots (h = even) could be the consequence of double diffraction. However, the *fourth* order satellite spots would also come in this position. It can therefore not be excluded that we are in fact observing satellites of even order only in this section.

The ideal structure, i.e., the structure as proposed by Tunell and Pauling (*1*) without modulations does not occur at room temperature. On heating up to melting or cooling down to liquid nitrogen temperature no changes in the diffraction pattern are noted; the modulated structure thus seems to be an inherent feature of the calaverite structure in a wide temperature range.

It is worth noting that for the hypothetical corresponding commensurate superstructure a superstructure spot would appear in the $h0l$ section at the nodes with h = odd, i.e., the intense second order satellite pair would fuse into a single spot. Also the 4.5 intervals in the $[13\bar{1}]^\star$ and $[10\bar{1}]^\star$ zones (Figs. 3a,b) would become equal to 4. This actually occurs in sylvanite.

In the $(h1l)^\star$ plane this hypothetical commensurate superstructure would produce a pattern of superstructure spots, formed by the first and second order satellites, which is the same as that found in the diffraction pattern of sylvanite. We shall discuss the possible significance of these remarks in Part II.

5. High Resolution Images

Bright field images were obtained along several relevant sections using an electron microscope operating at 200 kV with a C_s value of 1.2 mm and a theoretical resolution of 0.25 nm.

In Fig. 7 we reproduce structure images obtained along the [010] zone. The pseudo rectangular pattern of prominent bright dots corresponds in scale and orientation to the projected arrangement of gold atoms, i.e., the minority atoms of the calaverite structure. For certain thicknesses some of the rectangles contain pairs of somewhat less intense bright dots or elongated single dots, at the positions of tellurium columns. In other parts, i.e., under other contrast conditions, a rectangular arrangement of the same scale and orientation, but consisting of pairs of dots, becomes prominent; it corresponds to the arrangement of tellurium columns. The observed images are clearly in agreement with the structure of Fig. 1. When viewing the [010] images under grazing incidence long period modulations become obvious.

In the [010] zone two different modulation periods are revealed. The most prominent one corresponds with the wavevector $\bar{q}_1$ for which the satellite spots (i.e., the interfering beams) have the largest intensity. The second set of modulation waves, visi-

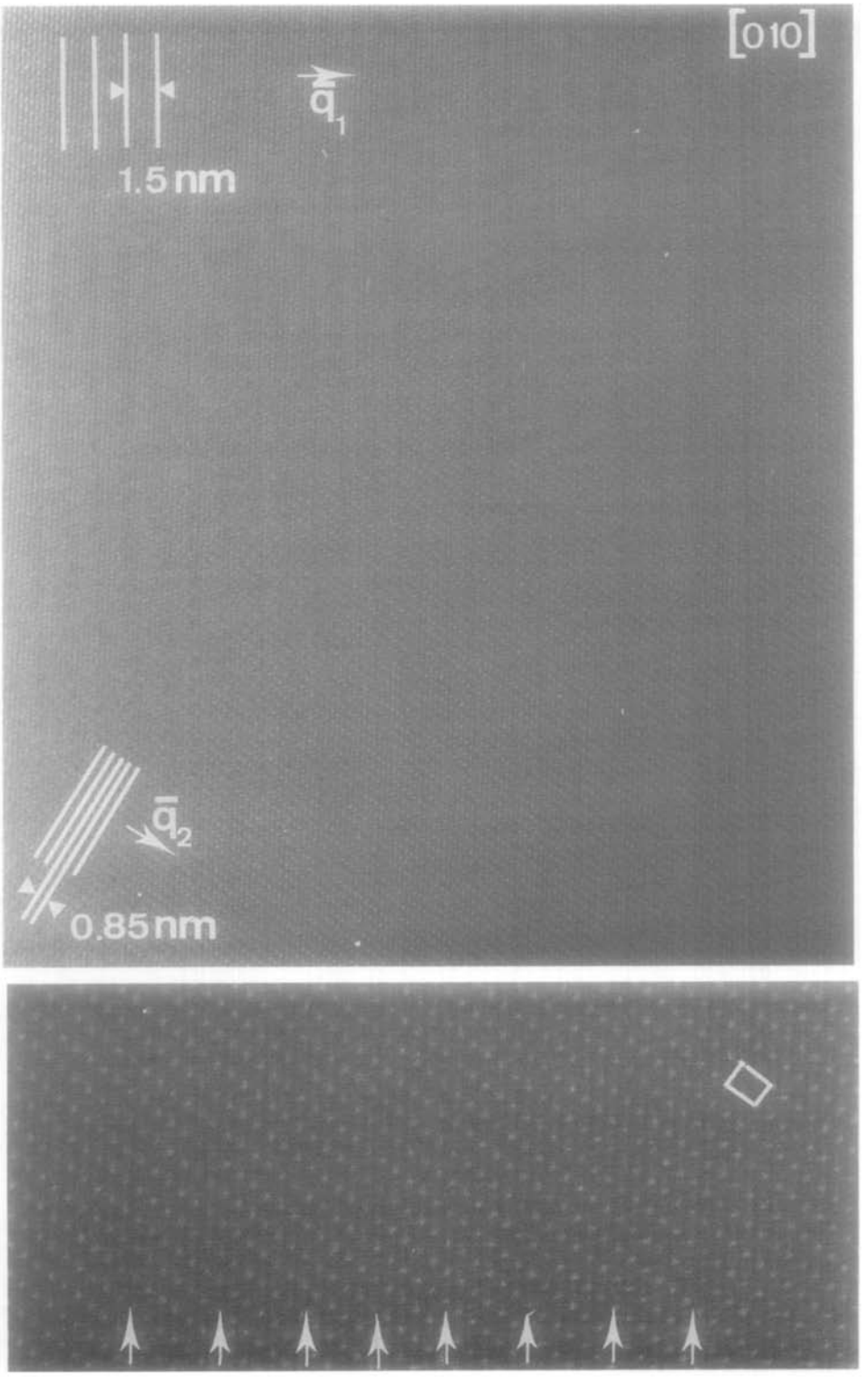
[010]
$\vec{q}_1$
1.5 nm
$\vec{q}_2$
0.85 nm

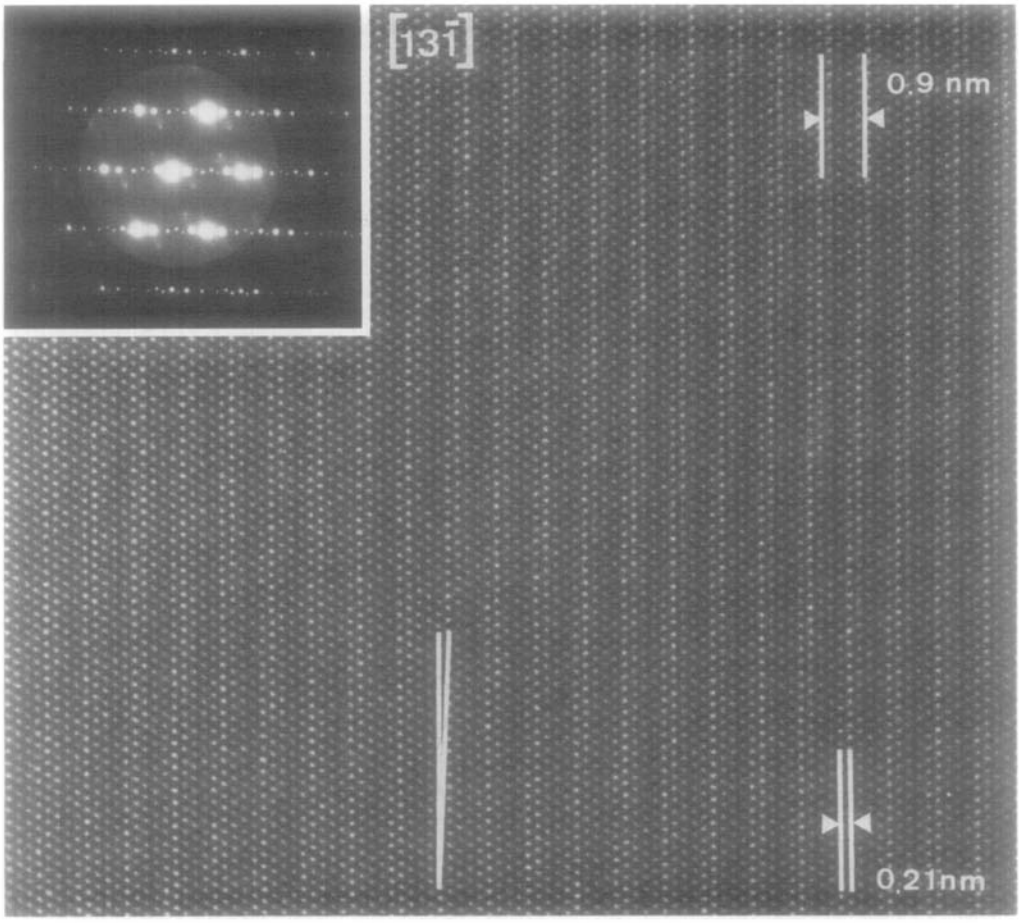

FIG. 8. High resolution image in the [13$\bar{1}$] section. The 0.94-nm modulation is very prominent. The diffraction pattern is shown as an inset. The rows of bright dots enclose a small angle with the close packed rows.

ble in the same image, corresponds with the vector $\bar{q}_2$. Further modulations are not observed in this section. The modulations described by larger $\bar{q}$ vectors are thus *not* revealed in this section presumably because the wavevectors are too large. We shall see that in the other sections the first order [202]* modulation becomes prominent.

Figure 8 shows the high resolution image along the [13$\bar{1}$] zone which is, roughly speaking, perpendicular to close packed planes. The pattern is very approximately ideally hexagonal. From the geometry alone it is not possible to conclude which atomic species is being imaged as bright dots; this can only be decided unambigu-

FIG. 7. High resolution images of the calaverite structure with the electron beam along [010]. (a) For a particular focus (≈−80 nm) and thickness (≈15 nm) a dot configuration resembling the projected structure is revealed, when associating bright dots with gold columns (see Fig. 9). The modulations in contrast have a wavelength corresponding with $\bar{q}_1$ and $\bar{q}_2$, respectively (see Fig. 6). (b) Enlargement of part of (a). A unit cell is indicated.

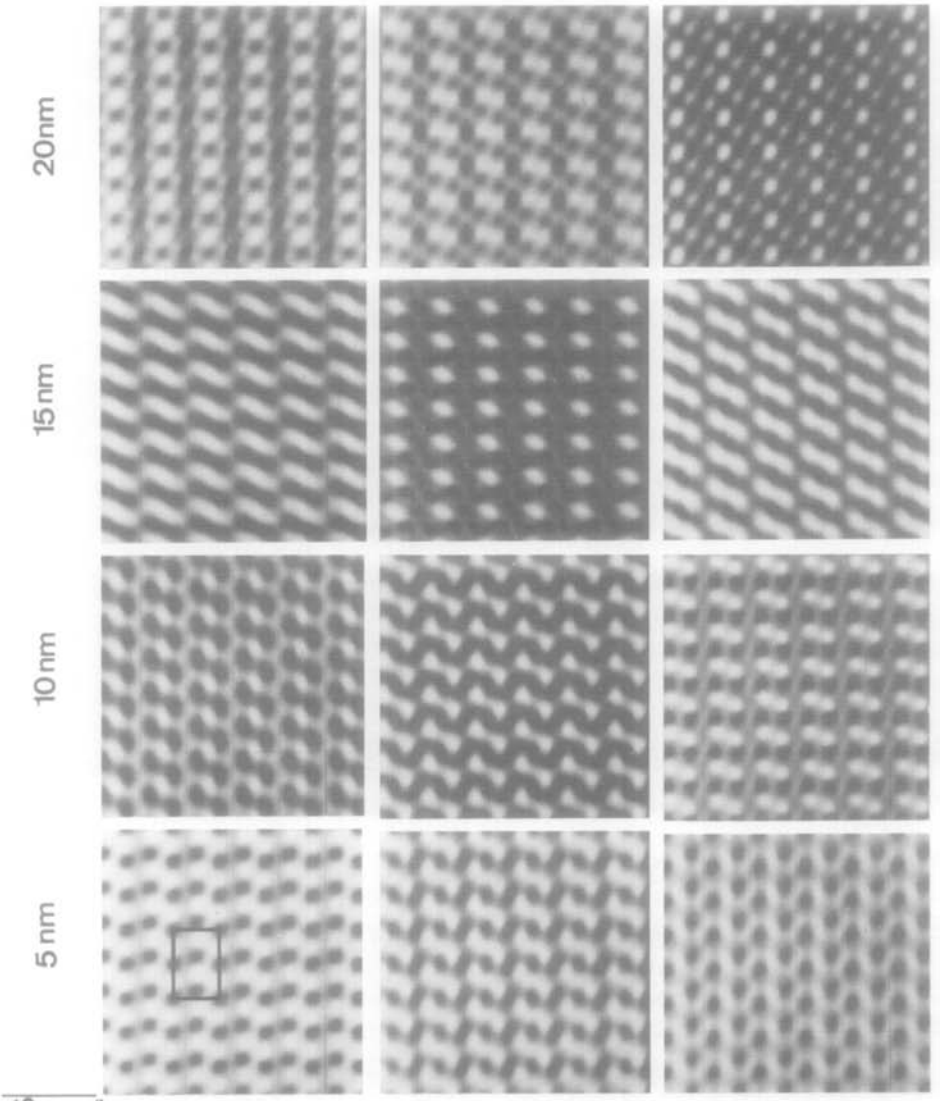

FIG. 9. Matrix of computed images along [010] for varying thickness and defocus values. The origin (lower left corner) is chosen to be a gold column). The calaverite unit cell is outlined.

ously on the basis of computed images. However, it is quite obvious that the arrangement of dots is strongly modulated in intensity; this is best visible in the thicker parts of the specimen. The direction of modulation encloses a small angle with a close packed direction of the dot pattern. The wave vector $\bar{q}$ characteristic of this modulation is indicated in Fig. 6. Since more than one satellite on each side of the basic spot is present in the diffraction pattern (Fig. 3) the modulation is not purely sinusoidal. From the diffraction pattern it is clear that the modulation is incommensurate with respect to the basic structure. This is also obvious from the image (Fig. 8); the rows of most intense spots contain systematic ledges, introducing a small orientation anomaly. The separation of homologous dense rows, which determines the superperiod, is not an integral number of separations between nearest neighbour rows, leading to a spacing anomaly.

The same modulation may occur in two variants differing roughly by 60° in orientation (Fig. 4). This modulation clearly reduces the true symmetry to triclinic. The modulations in the two variants do not need to have exactly the same period or the same orientation; this is evident from the diffraction pattern taken across two orientation variants of the same basic calaverite structure (Fig. 4 inset).

6. Image Simulations

We have produced simulated images of the ideal calaverite structure along different crystallographic directions. The method used was developed by D. Van Dyck (*4*). It fully takes into account dynamical diffraction effects as well as instrumental parameters. The output is plotted on a cathode ray screen, which produces an image of the same nature as the electron microscopic image. A matrix of simulated images, viewed along the [010] zone for different thickness and defocus values, is reproduced in Fig. 9. The best fit with the simplest observed image (Fig. 7b) is obtained for a thickness of 15 nm and a defocus of −80 nm. The lattice of bright dots clearly corresponds with the lattice of gold columns; however, the two lattices are displaced one with respect to the other over a vector $\frac{1}{2}[001]$, as is evident from the fact that in the simulated image the lower left corner corresponds with a gold position.

The observed images with resolved tellurium columns are best represented by the simulated image for a thickness of 20 nm and a defocus value of −100 nm. In this case the lattice of brightest dots represents the lattice of gold columns: the tellurium columns are represented as less bright dots. Again the actual configuration is shifted with respect to the simulated one.

In the simulated image for $t = 20$ nm and $\Delta f = -80$ nm on the other hand the atom columns are represented as dark dots; this image is practically the inverted version of the previously discussed one ($t = 20$ nm, $\Delta f = -100$ nm). The observed and computed images are now in phase if the dark dots are assimilated with Au-atom columns.

7. Selenium Substituted Calaverite

It was shown in (*5*) that up to 25% of the tellurium atoms in $AuTe_2$ can be replaced by selenium without modifying the structure to an appreciable extent. It was therefore considered of interest to examine the effect of such a substitution on the modulation vector. The doublet of satellites revealed in the [010] zone of calaverite is particularly sensitive to small changes in direction and magnitude of the modulation vector.

In pure $AuTe_2$ the direction of the doublet is almost exactly along the [201]* direction and the spacing corresponding with the distance between these spots is 14.5 ± 0.5 Å. In $AuTe_{1.75}Se_{0.25}$, on the other hand, the

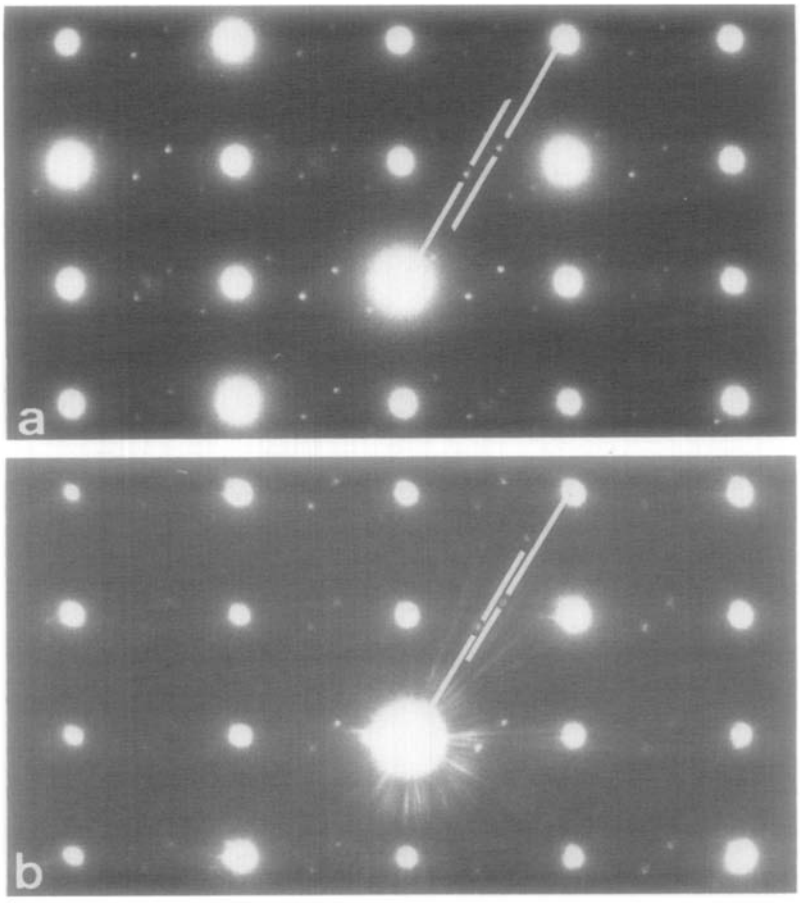

FIG. 10. Comparison of $\vec{q}$ vectors in (a) pure $AuTe_2$ ($1/q$ = 0.19 nm), and (b) $AuTe_{1.75}Se_{0.2}$ ($1/q$ = 0.925 nm).

direction is close to [302],* i.e., between [202]* and [201]* (Fig. 10), and the corresponding spacing is 17.1 ± 0.5 Å, i.e., significantly larger.

The inverse wavevectors of the modulation are $1/q$ = 0.94 nm in pure calaverite and $1/q$ = 0.925 nm in $AuTe_{1.75}Se_{0.25}$.

8. Discussion

The absence of the first order satellites in the [010] zone diffraction pattern, and of the associated modulation in the corresponding image, can be understood if it is assumed that the deviations from the ideal structure, described by the first harmonic in the modulation wave, result from displacements in the [010] direction, i.e., the polarization vector is along [010]; if these were the only displacements no satellites would be observed in the [010] zone. The fact that the second order (and possibly the fourth order) satellites are observed suggests that the second harmonic describes a displacement wave with a component *parallel* with the (010) plane, i.e., with a polarization vector having a component parallel with the (010) plane.

Our observations are at variance with the results of the X-ray diffraction study of Ref.

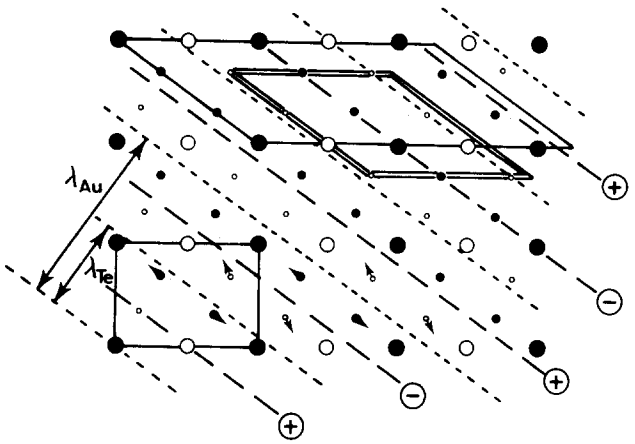

FIG. 11. Qualitative model for the modulated structure of calaverite. The unit mesh of the displacement pattern for gold is outlined in full line; the corresponding unit mesh for tellurium is outlined by double lines. This model is suggested by the commensurate structure of sylvanite (*1*). The gold atoms located closest to dashed lines marked + are displaced upwards in the [010] direction; those located closest to dashed lines marked − are displaced downards in the same direction. The other gold atoms closest to dotted lines remain at their level in the ideal structure. The tellurium atoms are displaced from their ideal positions as indicated for some of them in an exaggerated way by the arrows.

(*2*). From Ref. (*2*) it is not clear which are the planes of equal phase of the modulation. Our observations show that they are approximately the (101) planes, according to the description of Tunell and Pauling. These planes are indicated in Fig. 1. We also found a somewhat different orientation of the wavevector (an angle of 35° with $c^\star$ instead of 28°) as well as a slightly different length, $1/q = 0.94$ nm instead of $1/q = 0.83$ nm. Moreover the model proposed by the authors of (*2*) is apparently too simple since they assumed *all* displacements to be along the [010] direction.

Since in a number of sections several satellites are visible, the sinusoidal modulation, as discussed in Ref. (*2*), is only a rough approximation.

Also at variance with (*2*), we did find a small dependence of the satellite configuration on the silver content; this may explain part of the discrepancies concerning the wavevector since Sueno *et al.* used natural calaverite containing some silver, whereas we used pure synthetic $AuTe_2$.

A possible qualitative model for the (202) modulations in the calaverite structure should be consistent with the following observations.

The period of the modulations resulting from displacements in the [010] direction should be equal to ~4.5 times the distance between successive (101) planes, whereas the period of the modulation due to displacements parallel with the (010) plane should be equal to half of this distance, i.e., to 2.25 times the distance between successive (101) planes. The two modulation waves are thus closely coupled; they have parallel wavevectors of a length related by a factor of two and have a different polarization vector.

The structure of commensurate sylvanite, described in Ref. (*1*), and in which the silver positions as well as the gold positions would all be occupied by gold, is a possible modulated version of the ideal calaverite structure satisfying these requirements. However, in commensurate sylvanite the periods would be 4 and 2, re-

spectively, instead of ~4.5 and ~2.25; it is easy to visualize similar modulation waves along the same lattice planes with these incommensurate wavelengths. A model for such a structure is represented schematically in Fig. 11. The unit mesh of the displacement pattern for gold is outlined in full line; the corresponding unit mesh for tellurium is outlined by double lines. The dashed and dotted lines mark the extrema and the zeros, respectively, of the displacement wave for Au. The gold atoms located closest to dashed lines marked + are displaced upwards in the [010] direction; those located closest to dashed lines marked − are displaced downward in the same direction. The remaining gold atoms, closest to dotted lines, remain at their level in the ideal structure. The tellurium atoms are displaced from their ideal positions as indicated, for one unit mesh, in an exaggerated manner by means of arrows.

The electron diffraction patterns do not allow derivation of a quantitative model.

References

1. G. TUNELL AND L. PAULING, *Acta Crystallogr. 5*, 375 (1952).
2. S. SUNEO, M. KIMATA, AND M. OHMASA, AIP Conference Proceedings 53, "Modulated Structures 1979" (J. M. Cowley, J. B. Cohen, M. B. Salamon, and B. J. Wuensch, Eds.), p. 333.
3. G. VAN TENDELOO, R. WOLF, J. VAN LANDUYT, AND S. AMELINCKX, *Phys. Status Solidi A* **47**, 539 (1978).
4. D. VAN DYCK, *J. Microsc.* **119**, 141 (1980).
5. G. E. CRANTON AND R. D. HEYDING, *Canad. J. Chem.* **46**, 2637 (1968).